Supporting Information

Gipson et al. 10.1073/pnas.0913547107

SI Text

1. Ludtke SJ, Baldwin PR, Chiu W (1999) EMAN: Semiautomated software for high-resolution single-particle reconstructions. *J Struct Biol* 128:82–97.
2. Böttcher B, Wynne SA, Crowther RA (1997) Determination of the fold of the core protein of hepatitis B virus by electron cryomicroscopy. *Nature* 386:88–91.
3. Rosenthal P, Henderson R (2003) Optimal determination of particle orientation, absolute hand, and contrast loss in single-particle electron cryomicroscopy. *J Mol Biol* 333:721–745.
4. Johansson P, et al. (2008) Inhibition of the fungal fatty acid synthase type I multienzyme complex. *Proc Natl Acad Sci USA* 105(35):12803–12808.
5. Jenni S, et al. (2007) Structure of fungal fatty acid synthase and implications for iterative substrate shuttling. *Science* 316:254–261.
6. Johansson P, et al. (2009) Multimeric options for the auto-activation of the fungal FAS type I megasynthase. *Structure* 17(8):1063–1074.
7. Kelley LA, Sternberg MJ (2009) Protein structure prediction on the Web: A case study using the Phyre server. *Nat Protoc* 4:363–371.

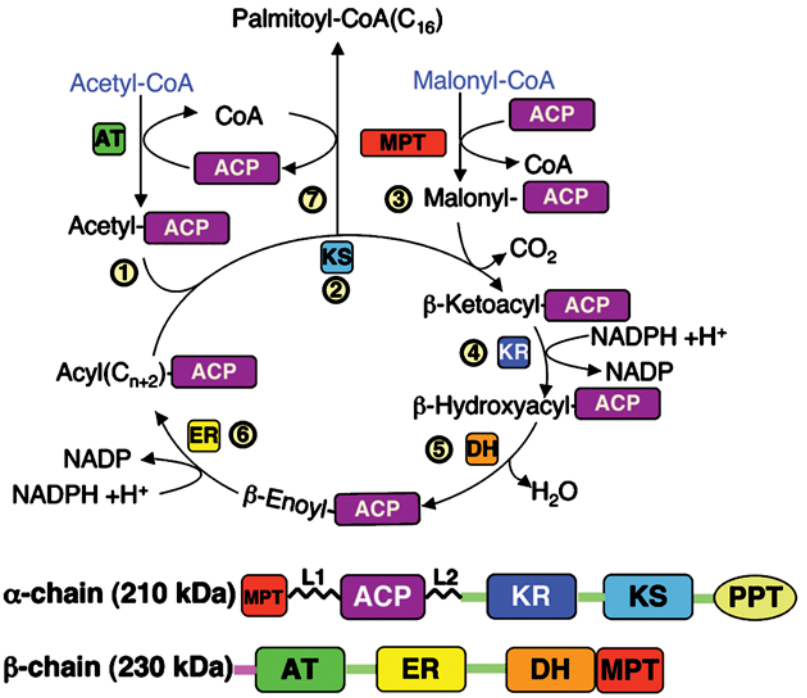

Fig. S1. Fatty acid synthesis reaction cycle. The coloring scheme for domains is the one used in the main figures. Numbers denote the steps in the fatty acid chain elongation cycle as follows: (1)(3) acetyl/malonyl transfer; (2) condensation; (4) ketoacyl reduction; (5) dehydration; (6) enoyl reduction.

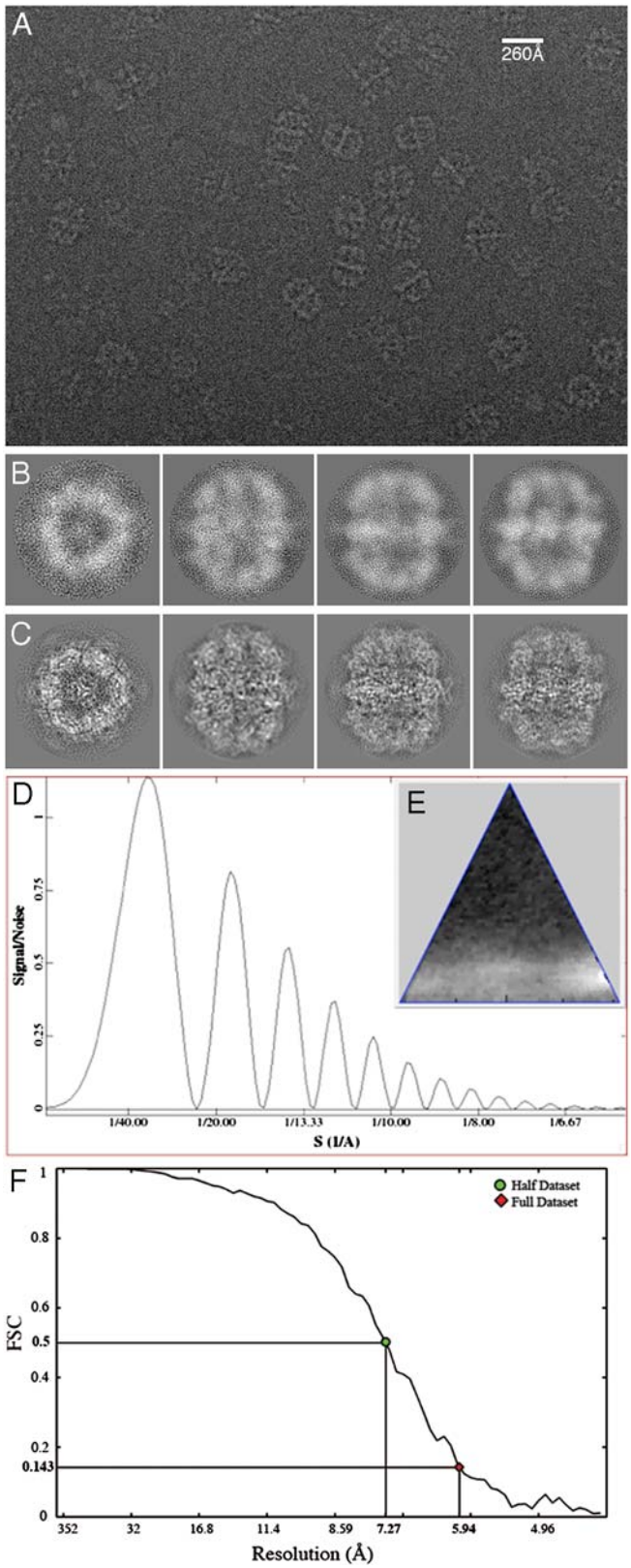

Fig. S2. Electron microscopy (EM) and image processing data. (*A*) Electron micrograph showing different orientations of fatty acid synthase (FAS) particles in vitreous ice (scale bar, 260 Å). (*B*) Representative class averages of characteristic top and side views with (*C*) corresponding map reprojections. (*D*) Signal-to-noise ratio plot of an image taken on film from the second dataset showing signal at subnanometer resolutions generated using CTFIT in EMAN (1). (*E*) Euler angle distribution of classified particles within the asymmetric triangle at an angular step size of 2° obtained from FAS data in EMAN. The brightness of each point indicates the number of particles present in the class average in that orientation. (*F*) Fourier shell correlation plot indicating map resolution at 0.5 cutoff (2) (7.2 Å; green) and at 0.143 cutoff (5.9 Å; red) (3).

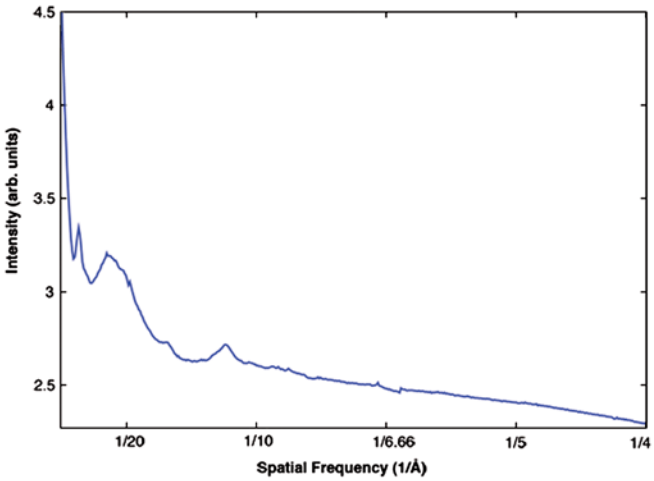

Fig. S3. (*A*) X-ray solution scattering curve for yeast FAS.

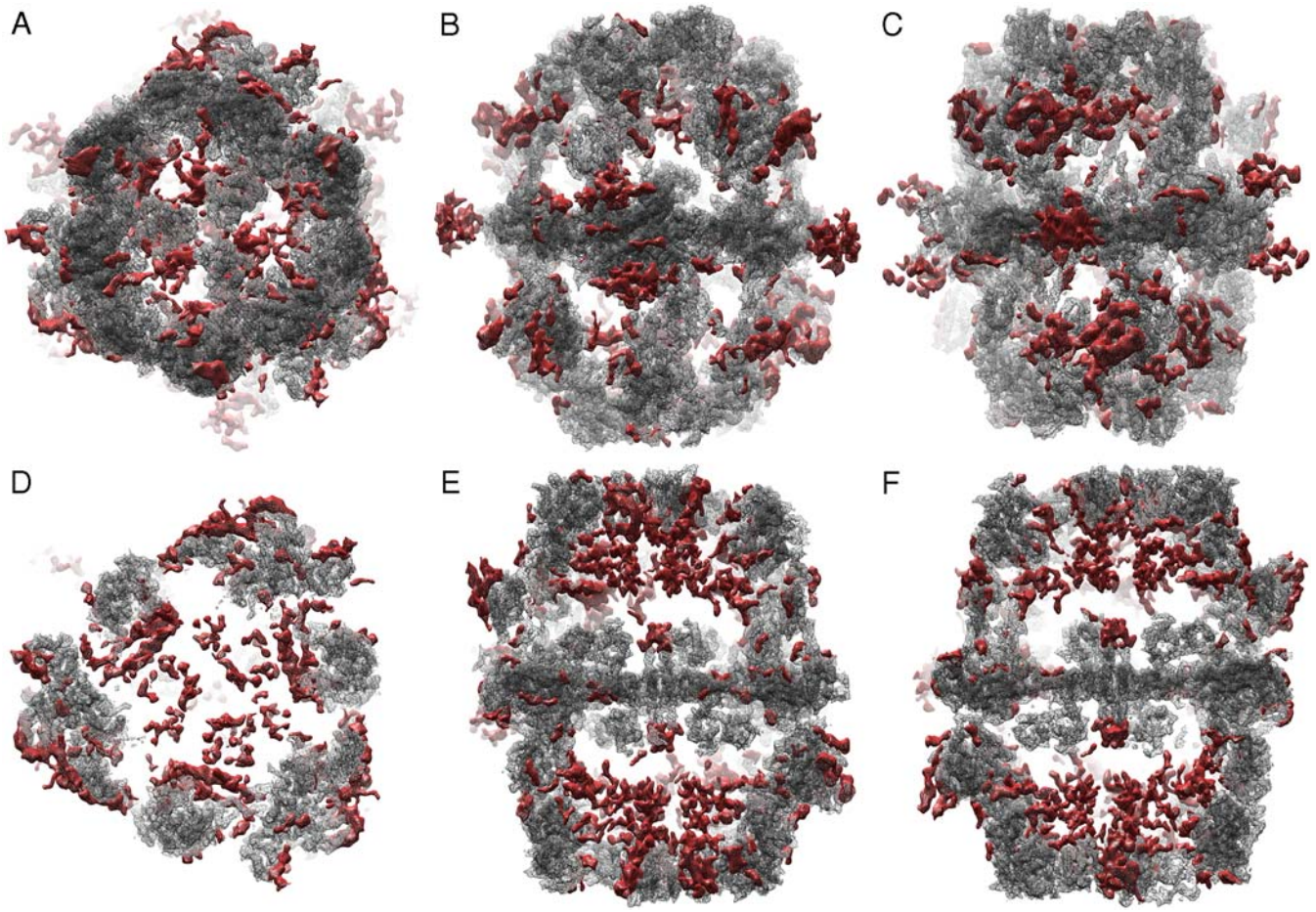

Fig. S4. Difference map between the EM map and the x-ray structure (2VKZ). The EM map and the x-ray structure of 2VKZ were filtered to 6 Å and normalized to calculate a difference map between the two structures. The electron density of the x-ray model is shown in gray mesh and the difference with the EM map in red mesh. *A*, *B*, and *C* represent the top view and two different side views, respectively, revealing differences in the barrel wall between the two structures, as well as features not seen in the x-ray structure outside the equatorial wheel. *D*, *E*, and *F* show sections of the map for the corresponding views in the top panel, revealing the differences in the barrel interior.

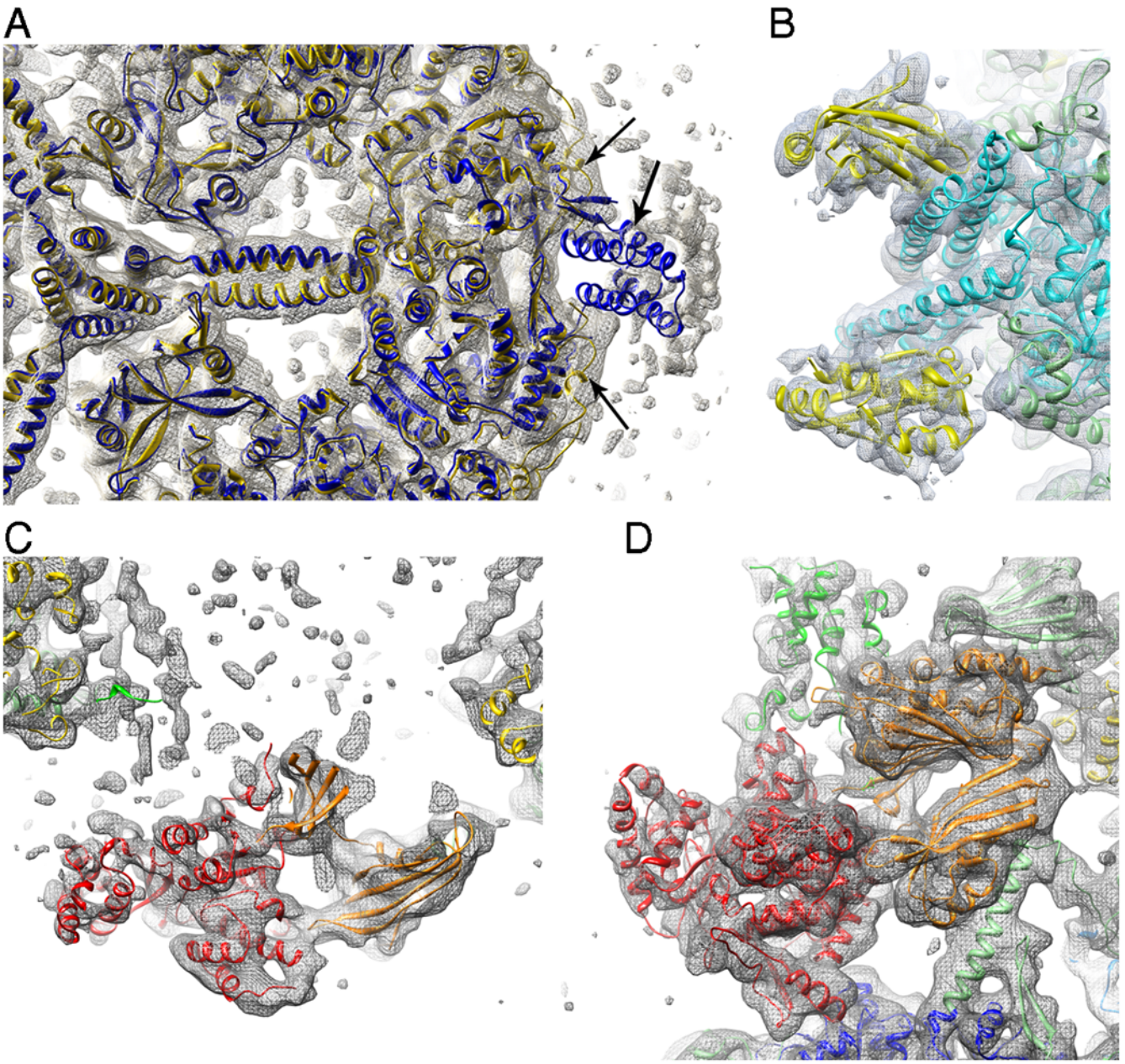

Fig. S5. The FAS EM map and fitted structure. (*A*) Complete structure of the α_6-wheel. The EM density is shown in white mesh, the yeast structure (2VKZ) (4) as a yellow ribbon, and the *Thermomyces* FAS (2UV9) (5) as a blue ribbon. Two arrows pointing toward the yellow ribbons indicate EM density and structure of the yeast model not present in *Thermomyces* FAS. The arrow toward the blue ribbon indicates the position of the ketoacyl reductase (KR) four-helix bundle seen in the *Thermomyces* x-ray structure, while the corresponding density in the EM map is seen in a horizontal position. (*B*) Fit of the phosphopantetheinyl transferase domain (yellow) (2WAS) (6) to the EM density (white mesh) at the ketoacyl synthase (KS) dimer (cyan). (*C*, *D*) Fitting of the malonyl-palmitoyl transferase (MPT) domain (red), which is mainly α-helical, and the dehydratase (DH) domain (orange), which is rich in β-sheet. The view in *C* shows a slice through the barrel, perpendicular to the 3-fold axis, and in *D* a side view of the barrel.

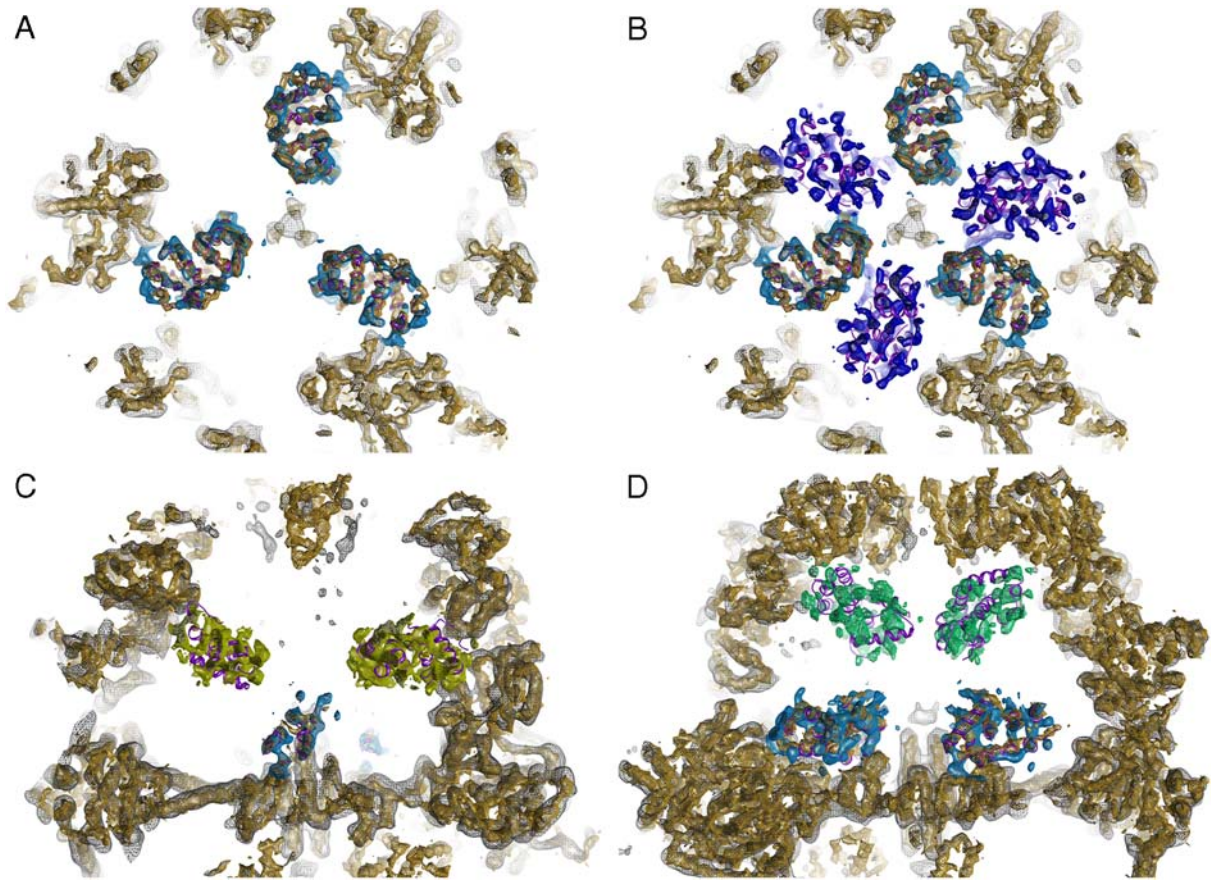

Fig. S6. The acyl carrier protein (ACP) model fitted to the EM density. The electron density of the x-ray structure (2VKZ) calculated to 6 Å is shown in gold mesh and the EM map in gray mesh. The ACP atomic model (purple ribbon) was fitted into the corresponding EM densities near the enzymatic domains, which are shown in color: KS (*A*, *B*, *D*) cyan, KR (*B*), blue, enoyl reductase (ER) (*C*), yellow, and acetyl transferase (AT) (*D*), green.

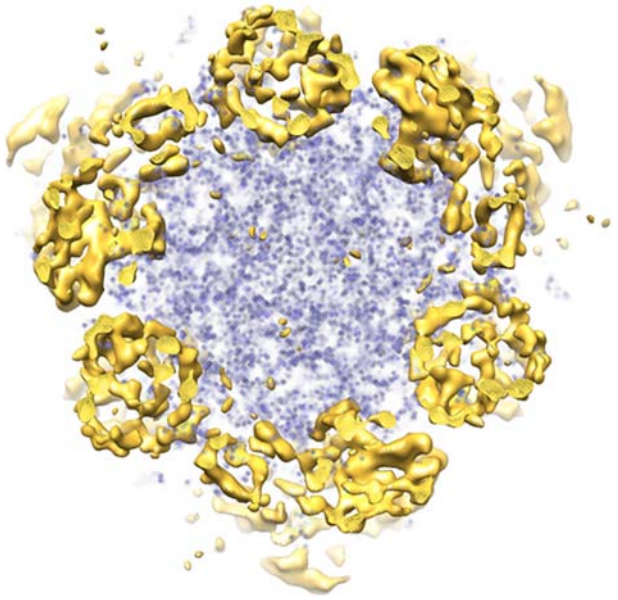

Fig. S7. Slice (20 Å thick) of the three-dimensional variance map (light blue) of the EM FAS structure (yellow) as seen from the top of the barrel.

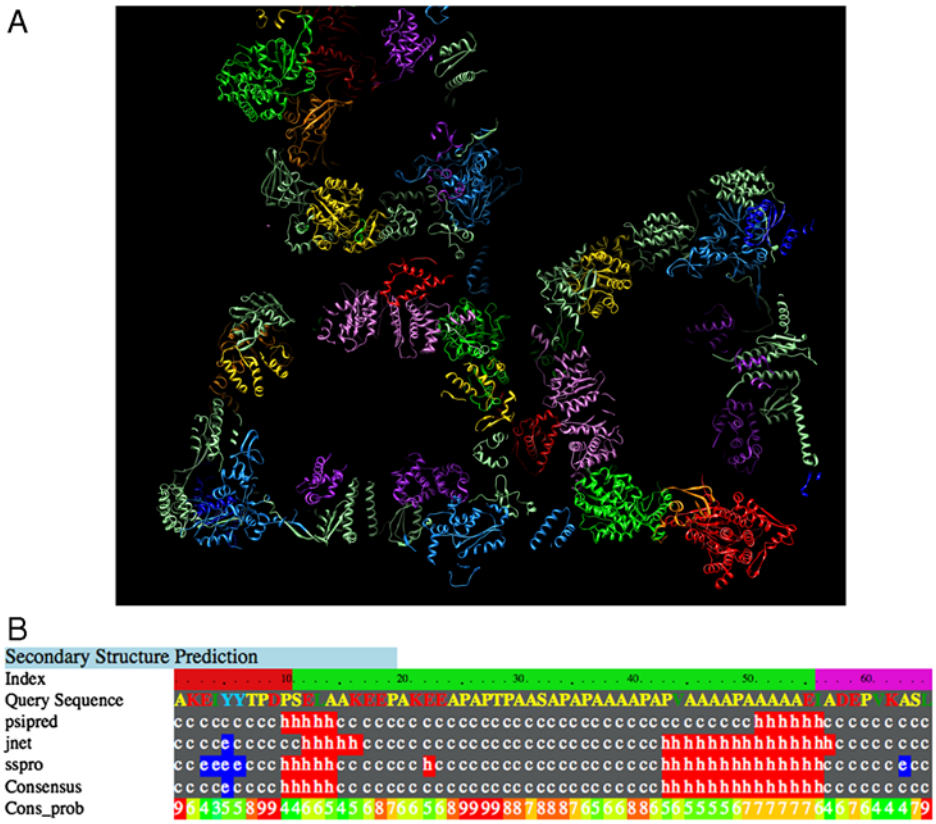

Fig. S8. (*A*) A slice view of 45-Å thickness showing the crystal contacts seen in all crystals of yeast and *Thermomyces* FAS. Crystal contacts involve the MPT domain (red) and the trimerization domain (pink). (*B*) Secondary structure prediction of the peripheral ACP linker, obtained from the Phyre server (7). The linker sequence is shown below the green bar, while the neighboring MPT and ACP domains are presented below red and purple bars, respectively. c: coil, h: α-helix, e: β-sheet.

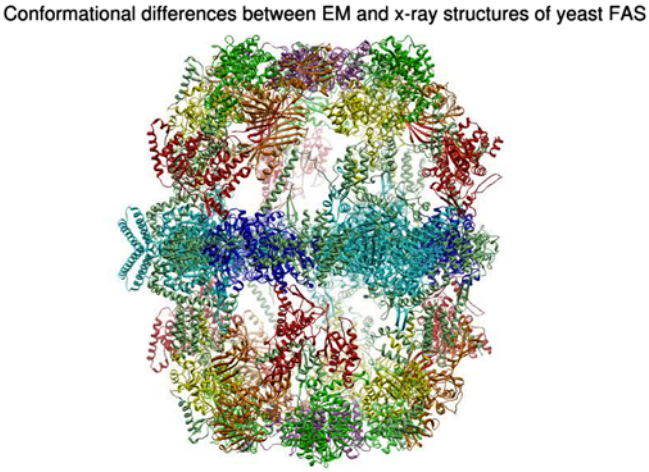

Movie S1. Conformational differences between the EM and x-ray structure of yeast FAS. The movie shows the x-ray model (2VKZ) alternating with the model based on the cryo-EM map. The color scheme shows AT (green), DH (orange), ER (yellow), MPT (red), KS (cyan), KR (blue), the structural domain near the 3-fold axis at the top of the dome (pink), the other structural domains (light green).

Movie S1 (MPG)

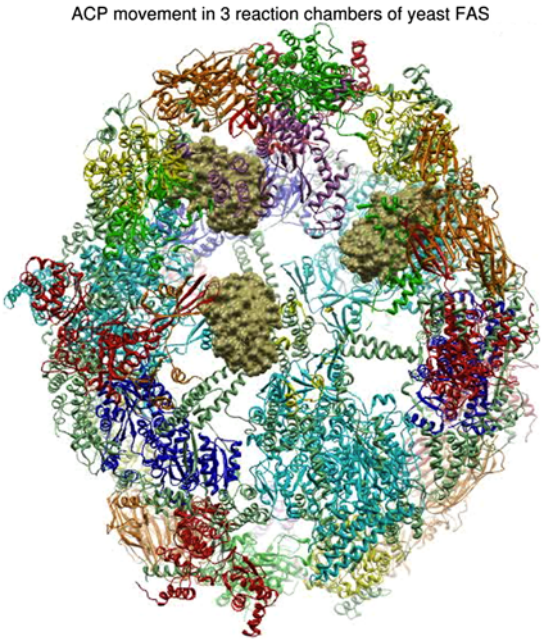

Movie S2. The positions of the ACP domain docked at the AT (green), ER (yellow), KS (cyan), and KR (blue) catalytic domains inside the three reaction chambers in one dome of yeast FAS. The ACP domain is colored corresponding to the catalytic domain it is docked to.

Movie S2 (MPG)